NdFeB VERSUS FERRITE IPM MOTOR FOR AUTOMOTIVE A.C. COMPRESSOR ELECTRIC DRIVING: MODELING AND FEM-EMBEDDED OPTIMAL DESIGN

Andy ISFANUTI, Lucian TUTELEA, Sorin AGARLITA, Ion BOLDEA
Dept. of Electrical Machines&Drives,"Politehnica" University of Timisoara, Bd. V. Pârvan, no.2, Timișoara, RO

Abstract: *Automotive a.c. compressor, for an average of 2kW at 6000 rpm, constitutes a major power automotive consumer; its electrification by a high efficiency (above 90%) variable speed drive is claimed to produce at least 33% energy savings. High energy (NdFeB) PMSM with surface and interior PM rotors have been tried for the purpose, for a motor efficiency above 93 - 94% which, for a PWM converter efficiency of 96%, would meet the typical 90% drive efficiency automotive requirements. However, the problem is the high recent price of sintered NdFeB permanent magnets. In view of automotive intensive electrification recent trends, the present paper investigates the performance of a dual (axial and radial) PM flux concentration Ferrite IPM (B_r=0.45T) rotor versus NdFeB IPM (B_r=1.13T) rotor motor for such a demanding application. The main contributions of the paper include: a quasi 3D magnetic circuit nonlinear model of IPMSM with NdFeB (one piece/pole) and of a dual PM flux concentration spoke-Ferrite-IPM rotor 6 slot/8 pole SM; an optimal analytical design methodology with embedded 2D FEM to verify the average torque production automatically, (in axial and radial cross-section) FEM inquiries to obtain, by tapered airgap and 2-shifted-segments-rotor, a reasonable cogging torque and a pretty sinusoidal emf such that to yield less than 5% total full torque pulsations for sinusoidal (vector) current control.*
About the same 95% machine efficiency is obtained with both NdFeB and Ferrite IPM at 2kW, 6 krpm, 42Vdc, but with a 33% reduction in active material cost for a 30% heavier machine in the case of Ferrite PM rotor.

Key words: *automotive compressor, interior NdFeB and Ferrite permanent magnet, optimal design, magnetic circuit model, finite element method*

1. Introduction

Automobile (vehicular) electrification [1-5] is a strong trend here to stay due to energy savings, more controllability and better ride comfort.

The a.c. compressors are important energy consumers (2kW at 6000 rpm, typically), still driven from the came shaft of the ICE. A variable speed electric drive was calculated capable to produce about 33% energy savings in comparison to the mechanical drive if a higher than 14 V_{DC} (say 42 V_{DC} or more) electric power bus is made available on board of vehicle.

While earlier - 2 kW at 15 krpm, 42V_{DC} PMSM electric drives (93% motor efficiency) with surface and interior PM rotors have been proposed [6], more recently 2kW, 6000 rpm, 42 VDC are preferred due to direct driving of the a.c. compressor and thus better overall efficiency (at least 90% motor + converter + transmission, if any, efficiency) needed for large forecasted energy saving.

No flux weakening (constant power speed range) is required for such application and thus, for small rotor saliency, rather pure i_q vector control suffices for the entire speed range. Also all such solutions [6] refer to high energy (sintered) PM-rotor SMs. The recent strong increase of such magnets price to 150 USD/kg or so, due to their scarce availability in face of large future needs in vehicular and wind energy electric machines, puts the problem of alternative, less expensive, but high performance electric machine topologies. About 95% full power, full speed motor efficiency for the case in point is required.

In an effort to produce such a solution, this paper does the following:

Section 2

• chooses an IPM rotor PMSM with spoke-shape 8 poles Ferrite (B_r=0.45T) rotor that is longer than the stator stack [7]. The motor has 6 stator poles in order to keep low the cooper weight (coils) and losses for reasonable stator core and rotor losses (f_{1n}=400Hz for 2p=8 PM rotor poles at 6 krpm).

• uses twice 2D FEM to investigate the longer than stator rotor stack influence on total PM flux in the stator coils (axial flux concentration) and, respectively, the radial PM flux concentration with the spoke (radial) PMs (V shape with practically no standard rotor yoke).

Section 3

• uses 2D FEM to produce a rather sinusoidal emf and less than 5% total full-torque pulsations by using (axially) two rotor segments shifted by 7.5 mechanical degrees (half of cogging torque period).

Section 4

• introduces a 3D simplified but nonlinear magnetic circuit to portray analytically the flux distribution and calculate the dq model circuit parameters of the machine for both cases: NdFeB and Ferrite IPM rotor longer than the stator. Then the dq model is used in the optimal design code.

Section 5

• embeds FEMM 4.2 in the analytical optimal design methodology and code to make sure automatically that the average torque calculated analytically is met by FEM calculations via a dedicated term in the multiple term objective (cost) function that contains: initial cost,

loss capitalized cost, temperature, demagnetization and torque error penalty terms. E.m.f. correction factor in the analytical model is introduced, based on torque nonrealization error, to increase convergence in the optimization code.
Section 6
• it uses the optimal design MATLAB code developed on the occasion for the already stated case study and compares the performance of NdFeB and Ferrite IPM rotor topologies.

2. The proposed comparative topologies

This section starts with some empirical choices based on experience, to be then proven successful by 2D FEM.

As the aim of our study here is to produce a high efficiency PMSM drive (95% motor efficiency at 2 kW, 6 krpm, 42 VDC) with a convenient initial cost (active materials cost + framing materials cost + mover factoring cost) we choose the sintered NdFeB (B_r=1.13T) IPM rotor SM as the comparison basis (Fig. 1.a). The paralelipiphedic magnets are cheaper than pole-arch-shaped surface PMs and the stator mmf space harmonics induced rotor eddy currents in them are 10 times lower than for surface PMs, even in IPMSM topologies with tooth-wound stator coils [8]. Also we choose a tooth-wound stator to reduce the copper weight (and losses), frame length; and we keep the stator slots (coils) count low (at 6) to reduce the manufacturing costs.

In order to hope for similar (high) efficiency in Ferrite PM (B_r=0.45) rotor PMSM, the spoke (radially placed) shape is used in a yoke-less rotor (Fig. 1 b), with 2p=8 poles, to obtain at least 170% PM flux concentration; as this in not enough, for high efficiency, we prolong the rotor stack to produce axial PM flux concentration [7] (another 160% or so); but for this to happen, the stack length per PM pole pitch ratio has to be moderate and the diameter of the rotor has to be larger (in general) than 4-5 times the PM pole pitch.

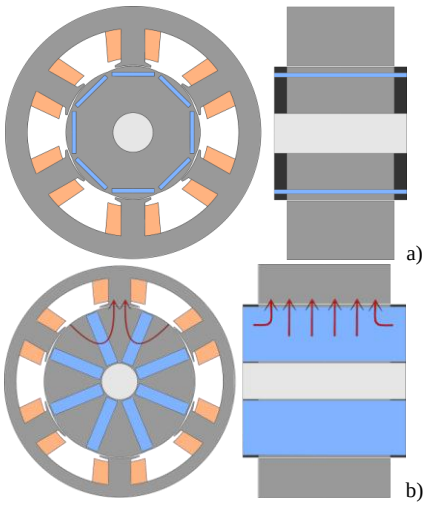

Fig. 1 Comparative NdFeB IPM rotor a) and Ferrite IPM rotor b) of 6 slot/8 pole synchronous motor

The rather small (5%) total full torque pulsations, not easy to obtain in the 6/8 configuration, is attempted here by, first tapered airgap with a reasonable PM span (thickness)/pole pitch ratio <0.3 and; second, by making the rotor of two segments shifted by 30° (electrical) that is 7.5° (mechanical).

3. FEM inquiries on Ferrite motor for sinusoidal EMF and axial PM flux concentration validation

In order to justify these rather daring choices we use here a tentative machine geometry (Table 1) obtained with 3D magnetic circuit model and circuit parameters developed, in fact, in the forthcoming paragraphs:

Table 1
Tentative machine geometry for 2D FEM inquiries

Parameter	Value	Description
Ns [-]	6	number of stator slots
poles [-]	8	number of rotor poles
Dso [mm]	70	stator outer diameter
Dsi [mm]	50	stator inner diameter
hag [mm]	0.4	airgap height
lstack[mm]	50	stack core length
hpm [mm]	3.5	PM height (thickness)
αsp [mm]	0.75	relative pole pitch width
swp [mm]	17	stator tooth width

First we use 2D FEM to calculate the axial PM flux concentration ratio versus the rotor length/stator stack length (Fig. 2) only to see a rather linear, but not proportional, rule, mainly due to magnetic saturation (μ - iron p.u. permeability).

The axial PM flux concentration ratio is used in the analytical model to calculate the magnetic permeance of axial rotor PM flux. The same info is used in the 2D FEM analysis in the radial plane to apply a virtual (increased) remanent flux density B_r' that "accounts for" the axial PM flux concentration effect.

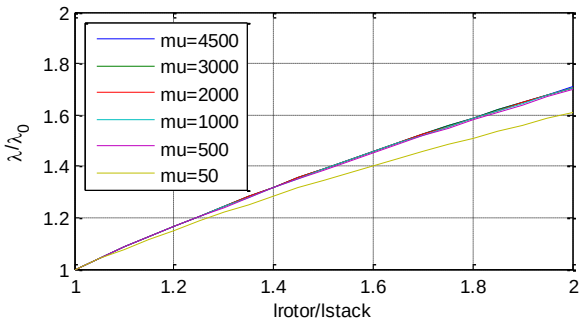

Fig. 2 Axial PM flux concentration ratio versus rotor/stator stack length

Further on, we do check the tapered airgap (g_{max}/g_{min}=2.0) influence on e.m.f. sinusoidality and on cogging torque, with no rotor skewing for the Ferrite IPM rotor (Fig. 3).

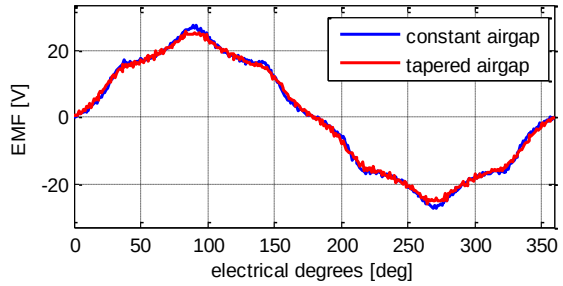

a)

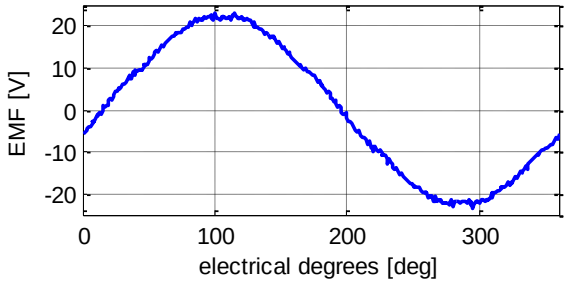

b)

Fig. 3 Emf for tapered and constant airgap for the Ferrite IPM straight rotor a) and skewed rotor (7.5°mechanical), b)

As the progress of tapered airgap is visible, the rotor making of two shifted segments is investigated by properly shifting the two rotor segments and the mmf phase to reduce full torque pulsations for rather full average torque calculated with given stator currents and geometry and for pure i_q control (Fig. 4)
The less than 5% total torque pulsations for sinusoidal pure i_q control is a strong argument to validate our rather empirical choices so far.
Not shown but done, the total torque versus rotor position for 100% current in phase A and -50% current in phase B and C, for the tapered airgap bi-segmental Ferrite IPM rotor, has its maximum very close to axis q (that is almost pure i_q control); this is another way to

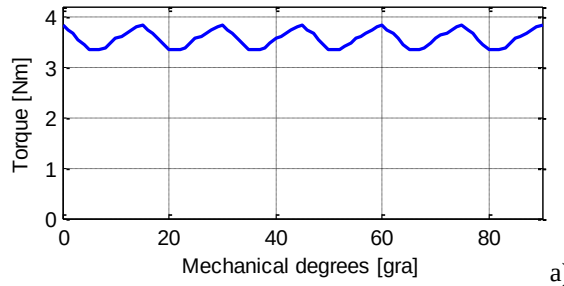

a)

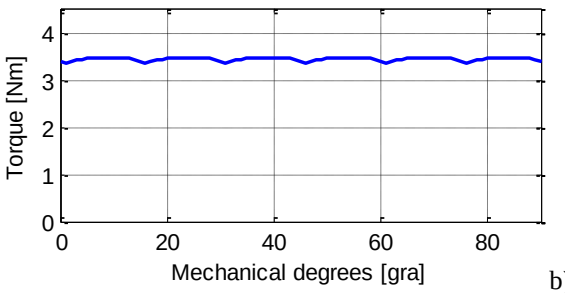

b)

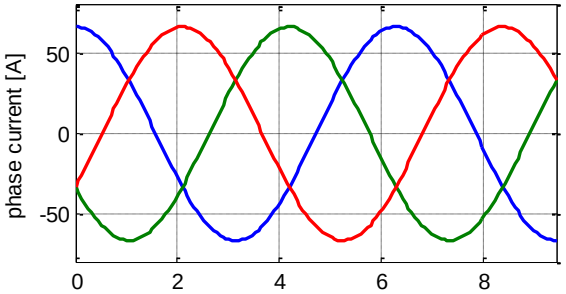

Fig. 4 Total full torque pulsations for Ferrite IPM rotor, with no skewing a), with two segments rotor (7.5° mechanical, shifting), b); phase current waveform c)

say that the machine saliency is small; this is beneficial as the reluctance torque in a tooth-wound standard (constant airgap, non-skewed rotor) is rather pulsating, due to the multitude of stator mmf space harmonics.

4. Proposed 3D magnetic circuit for Ferrite IPM rotor SM

The proposed simplified 3D magnetic nonlinear circuit for the Ferrite PM larger rotor is shown in Fig. 5. The axial PM flux permeance corrected by the FEM derived fringe factor R_{mrt} is essential here to consider the 3D character of rotor PM flux; which, then, becomes 2D when it enters the stator. The magnetic circuit is used to calculate iteratively (to consider magnetic saturation) the stator coil flux at zero and for given phase current instantaneous values; thus, finally, the standard nonlinear magnetization inductances L_{dm} and L_{qm} are computed; we add the standard leakage inductance to get L_d and L_q; also from the PM flux fundamental in the stator phase coils we calculate the emfs fundamentals.

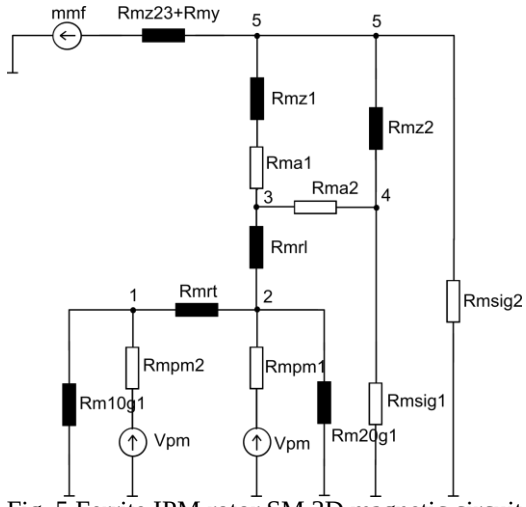

Fig. 5 Ferrite IPM rotor SM 3D magnetic circuit

R_{ma1} and R_{ma2} represent the airgap reluctances, while R_{msig1} and R_{msig2} stator slot flux leakage reluctances (all have constant values). R_{mz23} and R_{my} model the main tooth and yoke reluctance, passed by the same flux and R_{mz2} with R_{mz1} represents the bottom tooth reluctance. As for the rotor, the lines connected to node 1 model

the supplementary parts of the rotor, where R_{mrt} is the reluctance traversed by the flux which passes axially thorough the rotor core, R_{mpm1} and R_{mpm2} are PM reluctances (also having constant value), R_{m10g1} and R_{m10g2} represent the leakage reluctance for prolonged and main rotor part.

5. Optimal design methodology with embedded FEM

The optimal design methodology used here is adapted for the specific machine model considered here from Ref. [9]. It contains basically:

• eleven optimization variables defined as:

$$\bar{V}_{ar} = \left[\mathrm{Ds_i}\ \mathrm{Ds_o}\ s_{h4}\ s_{h3}\ s_{hy}\ s_{wp}\ h_{ag}\ h_{pm}\ l_{stack}\ \mathrm{dl_{pm}}\ \alpha_{sp} \right]^T \quad (1)$$

• the magnetic circuit derived L_d, L_q, and emfs expressions for the analytical nonlinear model and a simplified thermal model to eliminate "over-warm" designs through a dedicated penalty term in the optimal design code objective function.

• the multiterm objective (cost) function is:

$$\begin{aligned} f_{ob} &= c_i + c_e + c_p \\ c_i &= c_{\mathrm{cost}} + lam_{\mathrm{cost}} + PM_{\mathrm{cost}} + rot_{\mathrm{cost}} + pm_{\mathrm{cost}} \\ c_p &= c_{ptemp} + c_{pdemag} + c_{ptorque} \end{aligned} \quad (2)$$

where c_i is the initial cost, c_e - energy loss cost, c_p is the penalty costs. Initial cost contains copper cost (c_{cost}), lamination cost (c_{lam}), permanent magnet material cost (PM_{cost}), shaft iron cost (rot_{cost}) and passive (framing) materials cost (pm_{cost}). As for the penalty costs, c_{ptemp} is the penalty cost for over-temperature in stator windings, c_{pdemag} is the penalty cost for PMs demagnetization and $c_{ptorque}$ represents the penalty cost for the average torque nonrealization.

• the modified Hooke-Jeeves algorithm [10] is used in the optimal design dedicated MATLAB code.

• in order to make sure that the machine is capable to deliver the average torque forecasted by the analytical model in the optimal design, we check the total torque by two carefully chosen 2D FEM calculations of total torque that approximately contain its minimum and its maximum, to get an average for the machine with straight rotor; then the 2D FEM torque is compared to analytical torque for given i_q current and if the error is larger than ±5% the PM flux in the analytical model is corrected by an under-relaxation factor K_e dependent on the torque error:

$$K_e = 1 + \frac{k_{skewing} \cdot T_{FEM} - T_m}{T_m} \cdot 0.5 \quad (3)$$

This way not only a penalty function to correct the torque by FEM info is used, but, also, a means to correct the analytical model "on-line" is applied; consequently, faster convergence in optimal design is obtained. Also a 5% average torque reduction due to skewing is considered apriori in the analytical model.

Due to lack of space we stop here the description of the developed FEM-embedded optimal design methodology and continue with sample results.

6. Sample optimal design results for the case in point

For the design variable vector described in Table 2

Table 2.
Design variables with feasible domain of variation, initial and final values and initial variation step

Crt. No.	Design variable	Minimum value [mm]	Maximum value [mm]
1	Dsi	50	80
2	Dso	70	115
3	sh4	0.2	2
4	sh3	0.5	3
5	shy	4	10
6	swp	8	25
7	hag	0.4	1
8	hpm	1.5	6
9	lstack	20	65
10	dlpm	2	15
11	αsp	0.5	1
Crt. No.	**Initial value [mm]**	**Initial var. step [mm]**	**Final values [mm]**
1	70	7	76.2
2	100	10	115
3	1.2	0.12	0.4
4	2	0.2	0.5
5	8	0.8	5.9
6	17	1.7	11.1
7	0.4	0.04	0.5
8	3.5	0.35	6
9	50	5	65
10	7	0.7	7
11	0.75	0.075	0.5

a typical shorted, rather self-explanatory, design output file is given below:

```
% Electrical rated parameters
Pn=2000.000000; % W  - rated power
fn=400.000000;  % Hz - rated frequency
Vdc=42.000000;  % V  - dc voltage
In=46.583610;   % A  - rated current, rms value
mmfn=395.275038;    % A - coil rated mmf, peak value
fipm=0.000757;  % Wb - PM flux - no load, peak value per turn per coil
Rs=0.003464;        % Ohm - Winding Resistance
Ls=0.000060;        % H - Winding total inductance
Epm=23.364942;  % V - PM induced voltage per phase at rated speed
Pcu=22.552041;      % W - Rated copper loss
Pfe=60.171112;      % W - Rated iron loss
Pmec=20.000000;   % W - Mechanical loss (given in input file)
etan=0.951148;  %  - Rated efficiency
eta1=0.925972;  %  - Efficiency at rated torque and 0.300000 pu speed
Bagpm0=0.782047;    % T - air-gap PM flux density (peak value)
Bpm0=0.235114;  % T - PM flux density at zero current
Bpmn=0.155128;  % T - PM flux density at negative rated current in d axes

% Constructive dimensions
Dso=115.000000; % mm - Stator outer diameter
Dsi=76.200000;  % mm - Stator inner diameter
```

```
sh4=0.400000;   % mm - Stator tooth pole tip height
sh3=0.500000;   % mm - Stator wedge place height
shy=5.900000;   % mm - Stator yoke width
swp=11.100000;  % mm - Stator tooth width
hag=0.500000;   % mm - Air-gap height
hpm=6.000000;   % mm - PM height
lstack=65.000000;   % mm - Core stack length
dlpm=7.700000;  % mm - PM over-length
asp=0.500000;   % -  Relative pole pitch width
wpm=27.000000;  % mm - PM width
sh1=12.649816;  % mm - Stator coil height
sw1=41.687776;  % mm - Stator slot width (root)
sw2=28.990194;  % mm - Stator coil width (top)
sMs=19.673717;  % mm - Stator slot mouth
R1=39.000000;       % mm - Radius of tooth head  fig. 3.1
qw=14.479394;     % mm^2 - wire cross section
N1=6.000000;        %  Turns per coil
dcu=4.293686;    % mm - Wire equivalent diameter
lturn=181.735441;    %mm - Length of one coil turn
Dro=75.200000;   %mm - Rotor outer max diameter
Dro_min=74.148065;   %mm - Rotor outer min diameter

% Weights
mstiron=1.471480;   % kg - Stator core mass
mcu1=0.140991;  % kg - one coil copper mass
mcu=0.845949;   % kg - total cooper mass
mpm=0.510572;       % kg - total PM mass
mriron=1.944392;        % kg - Rotor iron mass
mst=2.317429;       % kg - Stator mass
mr=2.454965;        % kg - Rotor mass
mmotor=4.772393;    % kg -Motor total mass
Jr=0.00173537;  % kgm^2 - Rotor inertia

% Costs
cu_c=8.459486       % USD Copper cost
lam_c=11.179423 % USD Lamination cost
PM_c=3.063433       % USD PM cost
rotIron_c=0.861642  % USD PM cost
ac_cost=23.563984   % USD active material cost
pmw_c=8.113069  % USD passive material cost
i_cost=31.677053    % USD initial cost
energy_c=39.753801 % USD energy loss cost
t_cost=71.430854    % USD total cost
Opt_step=65.000000  % Optimization step
Opt_time=6690.799101    %s Optimization time

 % --------------------------------------------------------------------------

        %This output was produced using the next data as input:
% Primary Dimensions, Technical requests and Technological limitations

%Technical request
Pn=2000;    % W  - maximum power
fn=400; % Hz - base speed
Vdc=42; % V  - line voltage

%Primary Dimension
poles=8;        % number of poles
Nsc=6;      % number of stator tooth
nphase=3;   % number of phase
aa=1;       % parallel current path

%Initial values of Optimization dimension
Dso=100;    % mm - Stator outer diameter
Dsi=70; % mm - Stator inner diameter
sh4=1.2;    % mm - Stator tooth pole tip height- fig.3.1
sh3=2;  % mm - Stator wedge place height - fig.3.1
shy=8;  % mm - Stator yoke width
swp=17; % mm - Stator tooth width
hag=0.400000;   % mm - Air-gap height
hpm=3.5;    % mm - PM height
lstack=50;  % mm - Core stack length
dlpm=7; % mm - PM over-length
asp=0.75;   % -  Relative pole pitch width

%Optimization variable limitations
Dsi_min=50; % mm Minimum value of Stator inner diameter
Dso_min=70; % mm Minimum value of Stator outside diameter
sh4_min=0.2; % mm Minimum value of Stator tooth pole tip height
sh3_min=0.5; % mm Minimum value of Stator wedge place height
shy_min=4; % mm Minimum value of Stator yoke width
swp_min=8; % mm Minimum value of Stator tooth width
hag_min=0.4; % mm Minimum value of Air-gap height
hpm_min=1.5; % mm Minimum value of PM height
lstack_min=20; % mm Minimum value of Core stack length
dlpm_min=2;     %mm Minimum on side PM over-length
asp_min=0.5; % mm Minimum value of Stator open width

Dsi_max=80; % mm Maximum value of Stator inner diameter
Dso_max=115; % mm Maximum value of Stator outside diameter
sh4_max=2; % mm Maximum value of Stator tooth pole tip height
sh3_max=3; % mm Maximum value of Stator wedge place height
shy_max=10; % mm Maximum value of Stator yoke width
swp_max=25; % mm Maximum value of Stator tooth width
hag_max=1; % mm Maximum value of Air-gap height
hpm_max=6; % mm Maximum value of PM height
lstack_max=65; % mm Maximum value of Core stack length
dlpm_max=15;    %mm Maximum on side PM over-length
asp_max=1; % mm Maximum value of Stator open width

%Extra constraints
eta_min=0.93; % minimum efficiency at small speed and full torque
n1_pu=0.3;    % tipical speed
kn1=0.85;     % probability of the typical speed
kTmax=4;    % factor of overload torque
ksdemag=2; % demagnetisation safety coeficient

%Technological dimensions
sh1_min=2.5;   % mm - Minimum stator coil height
Dr_min=18;    % mm - Minimum shaft diameter
sMs_min=2.5; % mm - Maximum value of Stator open width
wbr1=0.5;   %
wbr2=1.5;   %
rhy_min=0.5;
wpm_pu=0.95; % - Relative PM width

d=1.2;      %coefficient to increase airgap in q axis
lc1=2;      % mm -straight part of coil end length
gphins=1;   % mm - inter phase insulation
kfill=0.4;   % slot filling factor
stcore='SURA007';   % Magnetic material data for stator / M19
rtcore='M19';  % Magnetic material data for
pm_material='FERRITE';      % Permanent magnet material

%Objective function coefficients
cu_pr=10; %USD/kg copper price
lam_pr=1.7; %USD/kg lamination price
PM_pr=6; %USD/kg PM price
rotIron_pr=1.7; %USD/kg - shaft iron price
energy_pr=0.5; %USD/kWh energy price (includes weighting factor in the
objective function)
pmw_pr=1.7; %USD/kg passive material price
hpy=1000; %h hour per year
ny=10; %years of use
kct=1; %over temperature penalty cost coefficient
kcdemag=1; %demagnetisation penalty cost coefficient
kfly=8; % weighting factor for inertia constraint in the objective function
(sept 16 2009)
kcT=15;% initial torque penalty cost coefficient

%Step size
d2=0.1*ones(1,11); d2(11)=0.002;        % mm - final step
ropt=2;     % optimization rate

% Other specification
Tw1=105; % deg. C - stator winding temperature
Tpm=100; % deg. C - rotor PM temperature
Tw_max=155; %deg.C - maximum winding temperature
Tamb=50; %deg.C - temperature of cooling fluid
alpha_t=14.2; %W/m^2*deg. thermal transmission coefficient
kff=3; %increasing factor of cooling surface
kT=1.05;% torque coefficient
kpfe=1.45; % iron losses factor (the iron loss are larger due to field non-
uniformity)
Pmec=0.01*Pn; % assumed mechanical losses
Pem_n=Pn+Pmec;  % W - maximum electromechanicall power
ktav=0.915; % Reduction factor of torque due to non-ideal magnetic field
distribution
k_skewing=0.95;% Reduction factor of torque due to rotor skewing
run_mode='o'; % Run mode: 'o' - optimization, 'e' - performances evaluation
finite_element_analysis=1; %'1' - for fem analysis, 0 for no analysis
output_file='output_42v.m'; % Name of the output file
t_file='output_42v.txt'; % Name of the table output file
trace_file='bldcipmm1'; % Name of the trace file for optimization
```

The evolution of four key geometrical variables during the optimization process is visible in Fig. 6.

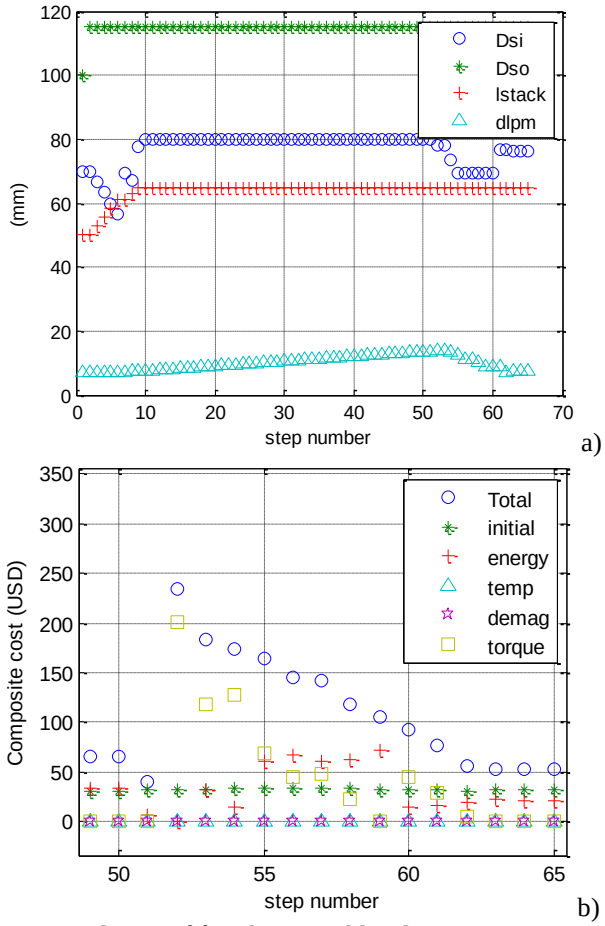

Fig. 6 Evolution of four key variables during optimization process of Ferrite IPM rotor SM a) and of its composite objective (cost) function b)

The efficiency, loss components and active weight evolution are depicted in Fig. 7 a, b, c.

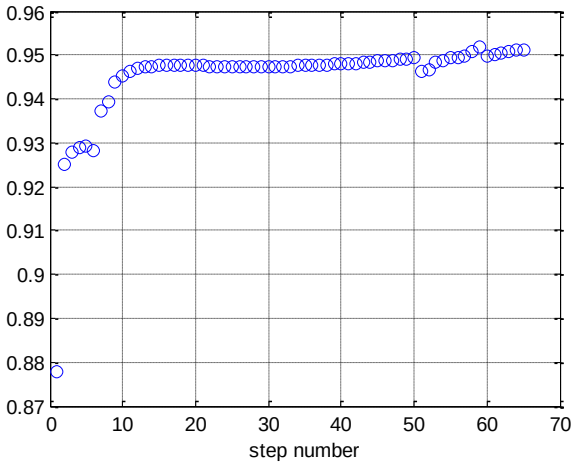

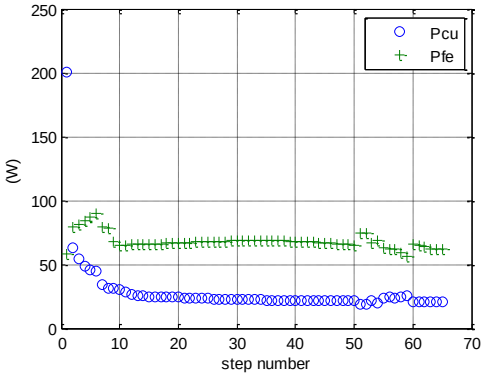

Fig. 7 Evolution of efficiency, a); loss components, b); active weight, c);

The results in Figs. 6 and 7 clearly indicate:

- a reasonable number of iterations
- the reaching of target efficiency (95%) for 2kW at 6 krpm and 42 V_{DC}
- the reasonable active weight of 4.6 kg (for high efficiency)
- a reasonable computation effort (111 minutes considering the embedded FEM inclusion)
- the fact that, due to rather high fundamental frequency (400 Hz at 6 krpm, 2kW), the iron losses are larger than copper losses. As intuitively the optimal efficiency is close to the situation where current and noncurrent losses are equal to each other, it seems that the use of low B_r (B_r=0.45) PMs has inevitably led to notably more iron and thus to more core losses in the design.

So far we did not show detailed optimal design results for the NdFeB IPM rotor SM due to lack of space; for more details see Ref. [11]. However, we present here in a synthetic manner a full comparison of optimal design output data for the NdFeB and Ferrite IPM rotor SMs considered in the investigation (Table 3)

Table 3
Optimal design results comparison: 2kW, 6 krpm

Para-meter	Unit	NdFeB PMSM	Ferrite PMSM	Description
Dso	mm	115	115	stator outer diameter
Dsi	mm	61.3	76.2	stator inner diameter
sh4	mm	0.8	0.4	stator tooth pole tip height
sh3	mm	0.9	0.5	stator wedge place height
sh1	mm	15.2	12.6	stator coil height
shy	mm	10	5.9	stator yoke width
swp	mm	10.7	11.1	stator tooth width

lstack	mm	48.1	65	core stack length
dlpm	mm	5.7	7.7	PM over-length
asp	-	0.5	0.5	relative pole pitch width
wpm	mm	19.095	27	PM width
sMs	mm	15.7	19.7	stator slot mouth
N1	-	7	6	number of turns per coil
dcu	mm	4.03	4.29	wire equivalent diameter (a few cond. in parallel)
lturn	mm	143.7	181.7	length of one coil turn
hpm	mm	1.9	6	PM height
hag	mm	0.4	0.5	air-gap height
mcu	g	685.93	845.95	copper mass
mstiron	g	1628.18	1471.48	stator iron mass
mlamin	g	4866.34	6576.13	lamination mass
mpm	g	132.97	510.57	PM mass
mriron	g	1265.89	1944.39	total rotor mass
mmotor	g	3712.98	4772.39	total motor mass
In	A	43.37	46.58	rated current
Vdc	V	42	42	input dc voltage
Rs	Ω	0.0036	0.0035	winding resistance
Ls	H	0.00056	0.00059	winding total inductance
Epm	V	25.67	23.36	PM induced voltage per phase
Psipm	Wb	0.01035	0.0090	total flux linkage per phase
Jr	kg•m^2	0.00064	0.00173	rotor inertia
Pcu	W	20.51	22.55	copper losses
Pfe	W	48.92	60.17	iron losses
Pmec	W	20	20	mechanical losses
etan	%	95.72	95.11	rated efficiency
eta1	%	93.03	92.59	efficiency at rated torque and 0.3 p.u. speed
cu_c	USD	6.859	8.459	copper cost
lam_c	USD	8.272	11.179	lamination cost
PM_c	USD	19.946	3.063	PM cost
rotIron_c	USD	0.553	0.861	rotor iron cost (shaft and partial iron)
ac_cost	USD	35.632	23.563	active material cost
pmw_c	USD	6.312	8.113	passive material cost
i_cost	USD	41.943	31.677	initial cost
energy_c	USD	0	39.753	energy penalty cost
t_cost	USD	41.943	71.430	total cost
Opt_step	-	26	65	optimization steps
Opt_time	s	4842.4	6690.7	optimization time

Also a comparison between key variables calculated with the analytical model and by 2D FEM is given in Table 4. They illustrate that, by and large, the nonlinear analytical model is capable to portray correctly the magnetic flux levels in the machine in the presence of the magnetic saturation.

Table 4.
Comparison between optimal design and FEM results

Para-meter	Optimal design value	FEM obtained value	Description
ϕ_1 [Wb]	$2.665 \cdot 10^{-4}$	$2.447 \cdot 10^{-4}$	magnetic flux in the airgap below half of main stator tooth
ϕ_2 [Wb]	$1.132 \cdot 10^{-4}$	$1.201 \cdot 10^{-4}$	magnetic flux in the stator tooth tip
ϕ_3 [Wb]	$3.787 \cdot 10^{-4}$	$3.666 \cdot 10^{-4}$	magnetic flux in the stator yoke
Bs_1 [Wb]	0.735	0.680	average flux density in the airgap below half of main stator tooth
Bs_2 [Wb]	1.934	2.030	average flux density in the tooth tip
Bs_3 [Wb]	0.985	0.955	average flux density in the stator yoke
Bs_4 [Wb]	1.047	1.035	average flux density in the middle of the stator tooth
E_{PM} [V]	23.36	22.08	PM induced voltage per phase at rated speed (peak value)
T [Nm]	3.18	3.45	total torque average value

The comparison reveals information such as:
• the outer stator diameter Ds_o was kept constant at 115 mm

• the stator bore diameter ended up as 61.3 mm for the NdFeB and 76.2 mm for the Ferrite rotor.
• the stator stack length is only 48.1 mm for the NdFeB rotor and 65 mm for the Ferrite rotor.
• the rotor inertia is only $6.4 \bullet 10^{-4}$ kg•m^2 for the NdFeB rotor, but $1.73 \bullet 10^{-3}$ kg•m^2 for the Ferrite rotor
• the rated efficiency is 95.72% for the NdFeB rotor and 95.11% for the Ferrite rotor; also both rotors lead to almost 93% efficiency at full torque, but for 0.3 p.u. speed.
• the cost of active materials is 35.63 USD for the NdFeB rotor machine and only 23.563 USD for the Ferrite machine; this is the main advantage of the proposed (Ferrite PM) motor.
• the PM cost goes down from 19.966 USD to 3.063 USD

The prices of active materials in our study are: copper (10 USD/kg), 0.5 mm silicon laminations (1.7 USD/kg), sintered NdFeB (150 USD/kg), Ferrite PMs (6 USD/kg).

Conclusions

The present paper main final remarks are:

• the proposed Ferrite IPM rotor SM drive (2kW, 6 krpm, 42 VDC) is shown capable of 95% efficiency for 23 USD active material costs, for less than 5% total full torque pulsations obtained with pure iq vector control.
• the dual axial and radial Ferrite PM flux concentration which produces about 2.0 p.u. flux magnification is the key to such performance.
• the tapered airgap and the bi-segmental rotor are proven to lead to the less than 5% total torque pulsations for sinusoidal current control.
• a 3D simplified non-linear magnetic circuit is proposed to portray the new rotor topology and proven adequate by dual 2D FEM investigations.
• the optimal design methodology developed for the scope based on the 3D nonlinear magnetic circuit, contains, as embedded, key FEMM 4.2 calculations, a penalty function component and a correction factor to guarantee the analytically (dq model) calculated torque, within 111 minutes of total computation time on a typical desktop computer.

Acknowledgement

This work was partially supported by the strategic grant POSDRU/89/1.5/S/57649, Project ID 57649 (PERFORM-ERA), co-financed by the European Social Fund – Investing in People, within the Sectoral Operational Programme Human Resources Development 2007-2013.

References

1. Nasar, S. A., Unneweehr, L., *Electric vehicle technologies*, book, John Wiley, 1981
2. Ehsani, M., Gao Y., Gay S. E., Emadi A., *Modern electric, hybrid electric and fuel cell vehicles*, book, CRC Press, Florida, 2004
3. Emadi A., Lee Y. L. and Rajashekara K., *Power electronics and devices in electric, hybrid electric and plug-in HEV*, IEEE Trans. vol. E-58, no 6, 2008, pp. 2237-2245
4. Chan K. T., Chan C. C. and Lin C., *Overview of PM brushless devices for electric and hybrid electric vehicles* IEEE Trans. vol. E-55, no 6, 2008, pp. 2246-2257
5. Boldea I., Scridon S. *Automobile Electrification Trends*, Record of EVER - 2010, Monte Carlo
6. Murakawi H., Kataoka H., Honda I. *High efficiency brushless motor design for Air Conditioner of the next generation 42V vehicle*, Record of IEEE - IAS - 2001
7. Silva V. C., Nabeta S. I., Afonso M. A. M., Cardoso J. R., *Axial flux concentration technique applied to the design of permanent magnet motors: theoretical aspects and their numerical and experimental validation*, IEEE International Conference on Electric Machines and Drives pp.1988-1994, 15.05.2005
8. Yamazaki K., Kamon Y., Fukushima Y., Ohki S., Nezu A., Kemi T. I. and Mizokami R., *Reduction of magnet eddy-current loss in interior PMSMs with concentrated windings*, IEEE Trans. vol. IA - 46, no 1, 2010, pp. 196-205
9. Boldea I., Tutelea L., *Electric machines: steady state, transients and design*, book, Chapter 14, CRC Press, Taylor and Francis, 2010
10. Hooke R., Jeeves T. A., *Direct search solution of numerical and statistical problems*, J. ACM 8(2), 1961, pp. 212-229
11. Işfănuți A. *NdFeB versus Ferrite IPMSM for low power applications*, Diploma thesis (in English), upt.ro, 2012